第 5 卷 第 3 期　　航空动力学报　　Vol. 5 No. 3
1990 年 7 月　　**Journal of Aerospace Power**　　July. 1990

振荡叶栅气动性能实验研究

EXPERIMENTAL INVESTIGATION OF OSCILLATING CASCADE AERODYNAMICS

Daniel H. Buffum (*NASA Lewis Research Center*)
Sanford Fleeter (*Purdue University*)

ABSTRACT A series of experiments are performed in the NASA Lewis Transonic Oscillating Cascade Facility to provide fundamental data quantifying the high subsonic and transonic steady and oscillating aerodyna-
mics of a biconvex airfoil cascade at realistic reduced frequency values for all interblade phase angles. This is accomplished by developing and utilizing an unsteady aerodynamic influence coefficient technique in which only one cascaded airfoil is oscillated at a time. The vector summation of the resulting airfoil surface unsteady pressures measured on a dynamically instrumented airfoil enables the unsteady aerodynamics of an equivalent cascade with all airfoils oscillating at any specified interblade phase angle to be determined.

【摘要】 为了提供双凸翼型叶栅在所有叶间相位角及实际折合频率下高亚音和跨音定常和振荡气动性能的基本数据，在NASA 路易斯研究中心的跨音振荡叶栅试验设备上进行了一系列试验。为了进行该试验，研制出并使用了非定常气动影响系数法，即叶栅中一次只有一个翼型振荡，测出该振荡翼型与邻近静止翼型上非定常压力的矢量和，藉此就能确定在特定叶间相位角下相当于全部叶片振荡的叶栅的非定常气动性能。

INTRODUCTION

The ability to predict flutter has not kept pace with recent advances in the design of advanced turbomachines and propellers. As a result, the development of advanced unsteady aerodynamic cascade models is of current research interest. However, to both direct the development of these models as well as to evaluate these and existing models, fundamental oscillating cascade data are required. Unfortunately, relatively few experimental results are available, particularly at realistic high values of the reduced frequency in the high subsonic and transonic flow regimes. This is due to the inherent complexity of the experiments. Namely, measurements must be obtained not only for each steady flow condition and reduced frequency value, but also over a range of interblade phase angles β. Because these experiments are so time consuming, results are obtained only for a very limited number of specified β.

Oscillating cascade data may be obtained for all interblade phase angle values through simpler experiments. In particular, when the unsteady disturbances are small, as in flutter stability problems, an unsteady influence coefficient technique can be utilized. In this technique, only one airfoil in the cascade is oscillated, with the resulting airfoil surface unsteady pressure distributions measured on the oscillating airfoil and its stationary neighbors. The unsteady aerodynamics of an equivalent cascade with all airfoils oscillating at any specified interblade phase angle value is then determined through a vector summation of these influence coefficient data.

Several investigations have been directed at validation of this technique through correlation of unsteady aerodynamic influence coefficient results with corresponding oscillating cascade data acquired with all airfoils oscillating at specified interblade phase angles. Hanamura, Tanake and Yamaguchi obtained good results for such experiments in a water channel[1]. Davies and Whitehead[2] performed experiments in an annular cascade at high subsonic inlet conditions and reduced frequencies up to 0.1, but the measurements were limited to unsteady aerodynamic moment coefficients. The effect of oscillating both an isolated airfoil and three cascaded airfoils at low speed was studied by Tanaka, Yamamoto and Fujimoto[3]. Although a summation of the influence coefficients was not presented, the technique appears promising in regions of attached flow. For a subsonic compressible flow

This paper is received in January, 1990.

field, Buffum and Fleeter[4, 5] found good correlation of influence coefficient airfoil surface unsteady pressure distributions and corresponding data acquired with all airfoils oscillating at specific interblade phase angle values. In supersonic inlet Mach number experiments at ONERA[6], the summation of influence coefficients has been compared to data for a linear cascade with two airfoils oscillating.

In this paper, the steady and unsteady aerodynamics of a cascade of biconvex airfoils executing torsion mode oscillations are investigated for two incidence angles at high subsonic and transonic Mach numbers at realistic reduced frequency values. This is accomplished in the NASA Lewis Transonic Oscillating Cascade Facility by developing and utilizing an unsteady aerodynamic influence experimental technique. Detailed steady airfoil surface pressure distributions quantify the mean flow field. Unsteady airfoil surface pressure influence coefficients are measured for one oscillating airfoil in the cascade. These influence coefficents are then summed vectorally for correlation with data obtained with all airfoils oscillating at specified interblade phase angle values. The associated unsteady pressure difference data are also correlated with the predictions of a linearized subsonic oscillating cascade analysis.

INFLUENCE COEFFICIENT TECHNIQUE

Figure 1 depicts the two-dimensional finite thin airfoil cascade representation of a rotor blade row. For a given mean flow field and reduced frequency, the assumption of small unsteady disturbances allows the cascade unsteady aerodynamics to be expressed as lineary combined influence coefficients which can be determined both experimentally and analytically.

Consider a finite airfoil cascade with $2N+1$ airfoils executing constant amplitude harmonic oscillations with a constant β. The unsteady airfoil surface pressure, expressed as a pressure coefficient $C_p(x)$ acting at a point on the reference airfoil (Airfoil 0 in Figure 1), can be expressed as a Fourier series, Eq. 1. Thus these influence coefficients define the unsteady pressure coefficient developed on the reference airfoil due to the motion of airfoil n with all of the other airfoils stationary.

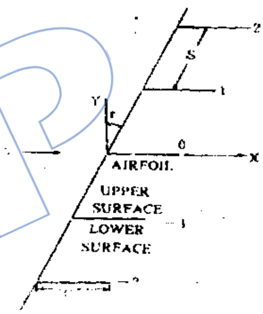

Figure 1. Cascade geometry

$$C_p(x, \beta) = \sum_{n=-N}^{N} C_p^n(x) e^{in\beta} \quad (1)$$

where C_p^n are the complex unsteady aerodynamic pressure influence coefficients.

OSCILLATING CASCADE FACILITY

The NASA Lewis Transonic Oscillating Cascade Facility, Figure 2, combines a linear cascade wind tunnel capable of test section inlet Mach numbers approaching unity with a high speed mechanical drive system which imparts controlled torsional oscillations to any or all of the airfoils. Air drawn from the atmosphere passes through a smoothly contracting inlet section, into a constant area 9.78 by 19.21cm test section and then through a diffuser and exhaust header. The flow rate is controlled by two valves located in the header. Upstream of the test section, a partitioned bleed system applies suction to the end wall boundary layers, thus reducing end wall viscous effects. Suction is also applied through tailboard slots to reduce effects due to the upper and lower cascade walls.

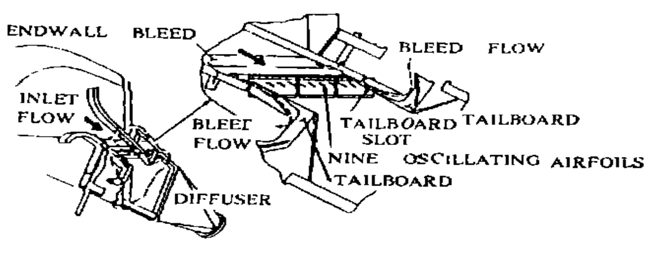

Figure 2. Cascade facilty

To obtain realistic values of the reduced freuqency, the mechanical drive system must provide high frequency controlled oscillations of the airfoils. Nine barrel cams, each with a six cycle sinusoidal groove machined into its periphery, are mounted on a common rotating shaft dirven by a 74.6kW electric motor. Connecting arms, joined to one end of each airfoil by trunnions, have buttons on the opposite end to follow the camshaft. The amplitude of the airfoil motion is 1.2 degrees, dictated by the cam and follower geometry. When all of the airfoils are oscillated, the various specified constant interblade phase angle airfoil oscillations are achieved by rotating the cams to new relative positions. In this investigation, the maximum airfoil oscillatory frequency is 350Hz, corresponding to a reduced freuqency of 0.39 with a 0.65 cascade inlet Mach number and 0.323 at Mach 0.80.

AIRFOILS AND INSTRUMENTATION

The cascade is comprised of nine uncambered biconvex airfoils with a chord of 7.62cm, a thickness-to-chord ratio of 0.076, a solidity of 1.3 and a 53 degree stagger angle. The radius of curvature of both airfoil surfaces is 27.4cm, with the leading and trailing edges rounded with a 0.025cm radius of curvature. The airfoils are supported by two midchord trunnions, resulting in a midchord elastic axis location.

Steady airfoil surface pressure distributions are measured with conventional static pressure taps. There are 16 chordwise measurement locations, with four additional taps to assure the spanwise uniformity of the pressure distribution. Rows of sidewall static pressure taps located upstream and downstream of the cascaded airfoils, Figure 2, are used to determine the mean inlet and exit static pressures.

The primary dynamic data quantify the complex unsteady surface pressures on the oscillating cascaded airfoils. These data are obtained via six Kulite dynamic pressure transducers flush mounted symmetrically about the midchord of one surface of the airfoil, as follows: AIRFOIL: Type- biconvex, no camber; Surface radius of curvature- 27.4cm; Leading and trailing edge radii of curvature- 0.025cm; Maximum airfoil thickness- 0.58cm; Chord C- 7.62cm; Elastic axis- midchord; Dynamic pressure transducer locations- 12, 25, 40, 60, 75, 88% chord. CASCADE: Number of airfoils- 9; Solidity C/S- 1.3; Spacing S- 5.86cm; Stagger angle γ- 53 degrees; Amplitude of motion- 1.2 degrees. These transducers, having an active sensor diameter of 0.097cm (1.3% of the airfoil chord), are placed in milled slots and potted in RTV for isolation from airfoil strain. A thin coating of RTV protects the sensor surface and fairs it into the surface contour of the airfoil.

The time-variant position of the reference oscillating airfoil is determined by a capacitance-type proximity sensor which produces a voltage proportional to the air gap between it and an adjacent object. This sensor is positioned to face a six cycle sinusoidally-shaped cam mounted on the airfoil drive camshaft so as to be in phase with the reference airfoil motion.

DATA ACQUISITON AND ANALYSIS

Conventional instrumentation is used to quantify the steady flow field. An average of the upstream sidewall static pressures along with the atmospheric pressure are used to calculate the inlet Ma. Steady flow airfoil surface static pressures are calculated from an average of about 100 samples.

Unsteady signals are a. c. coupled and recorded on magnetic tape for post-experiment processing. During tape playback, the signals are simultaneously digitized at rates sufficient to capture at least three harmonics of the oscillation frequency, with 32768 samples taken per channel. Each data channel is divided into blocks, typically with 4096 samples, and the Fourier decomposed and referenced to the airfoil motion by subtracting the motion phase from the unsteady pressure phase. With all of the signal blocks decomposed, the results are averaged and, for the influence coefficient data, the transducer acceleration calibration responses subtracted vectorally. To minimize errors due to spectral leakage, an interpolation scheme is applied to the decomposed results in conjunction with a Hanning window[7].

Final unsteady pressure data are defined by the complex dynamic pressure and pressure difference coeffcients, C_P and ΔC_P Equation 2. Dynamic pressure coefficients for any interblade phase angle are determined by summing influence coefficients per Equation 1.

$$C_p(x) = p_1(x)/(1/2)\rho V^2 \alpha_1 \quad ; \quad \Delta C_p = C_{p1} - C_{pu} \qquad (2)$$

where p_1 is the first harmonic of the unsteady static pressure, α_1 is the torsional oscillation amplitude and C_{p1} and C_{pu} are the lower and upper airfoil surface unsteady pressure coefficients.

RESULTS

The oscillating cascade aerodynamics are experimentally investigated at flow conditions defined by incidence angles of 0 and 7 degrees with an inlet Mach number Ma of 0.65 and 7 degrees incidence with Ma= 0.80. With the instrumented reference airfoil in Position 0 as defined in Figure 1, influence coefficient data are acquired on this airfoil with the airfoils in Positions − 2, − 1, 0, + 1 and + 2 individually oscillating at reduced frequencies of 0.390 for Ma= 0.65 and 0.323 for Ma= 0.8.

The steady airfoil surface pressure distributions are presented first, then the unsteady pressure influence coefficients on the individual surfaces of the reference instrumented airfoil are considered. These influence coefficient data are then summed to predict the unsteady aerodynamics of an equivalent cascade with all airfoils oscillating at a fixed interblade phase angle value. For several different interblade phase angles β, the resulting unsteady pressure distributions are correlated with: (1) baseline data obtained in experiments in which all of the airfoils were simultaneously oscillating at β= − 90°, 0° and + 90°; (2) predictions from the classical unsteady, small perturbation, subsonic, zero mean incidence flat plate analyses of references 8 and 9. Additional interblade phase angle results are obtained utilizing the influence coefficient technique and correlated with the flat cascade predictions. In these experiments, the airfoil motion is defined by the change in the incidence angle α with time:

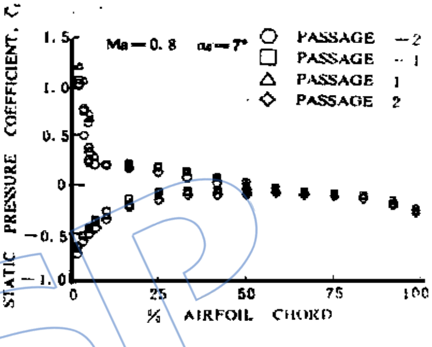

Figure 3. Periodicity of pressure distribution

$$\alpha(t) = \alpha_0 + \alpha_1 Re\{e^{(i\omega)}\} \qquad (3)$$

where α_0 is the mean steady α_1 is the oscillatory amplitude of 1.2 degrees and ω is the frequency.

Steady State Aerodynamics To demonstrate periodicity at the steady state conditions, airfoil surface pressure distributions were obtained for multiple passages in the cascade. For example, Figure 3 presents data at Ma= 0.8 for the four cascade passages surrounding the center airfoil. The Passage 1 data are the pressure distributions on the upper surface of Airfoil 0 (the center airfoil) and the lower surface of Airfoil 1; Passage − 1 data are for the lower surface of Airfoil 0 and the upper surface of Airfoil − 1, etc. The good cascade periodicity is readily apparent. Analogous results were obtained at Ma= 0.65.

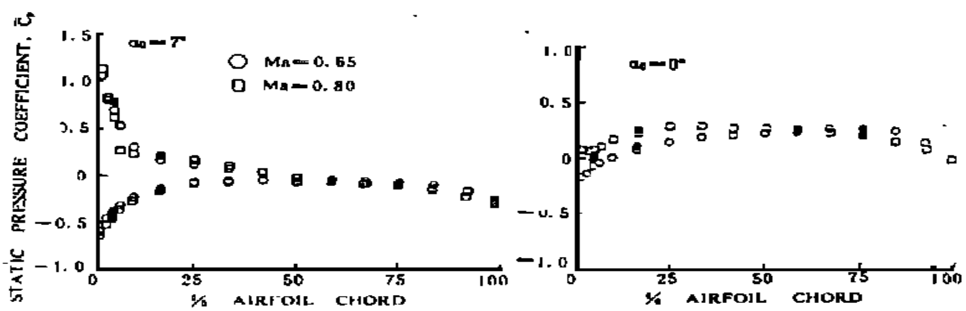

Figure 4. Steady flow airfoil surface pressure distribution

Figure 4 presents the steady flow airfoil surface pressure coefficient distributions on the center airfoil with the cascade mean flow incidence angle set at 0 and 7 degrees. The zero pressure difference conditions at the trailing edge is satisfied. Also, the pressure coefficient distributions are neary identical for the two Mach numbers, with loading only on the forward half. At $Ma = 0.8$, there is a small region of supersonic flow on the upper surface near the leading edge which is terminated by a shock, as determined from schlieren images.

UNSTEADY PRESSURE INFLUENCE COEFFICIENTS

Figures 5 presents the chordwise distribution of the unsteady pressure influence coefficients on the individual surfaces of the Position 0 reference airfoil, with the oscillating airfoil in the three relative positions defined by − 1 through + 1 at incidence and an inlet Mach number of 0.80.

The self-induced oscillating airfoil unsteady pressure response is shown in Figure 5a. Namely, this figure presents the unsteady pressures on the surfaces of the reference airfoil, with the reference airfoil itself oscillating. The magnitude of the unsteady pressure on each surface attains a maximum at the leading edge, tending towards zero at the trailing edge, with the magnitude generally larger on the upper surface. Also, the upper surface phase data are out-of-phase with the airfoil motion.

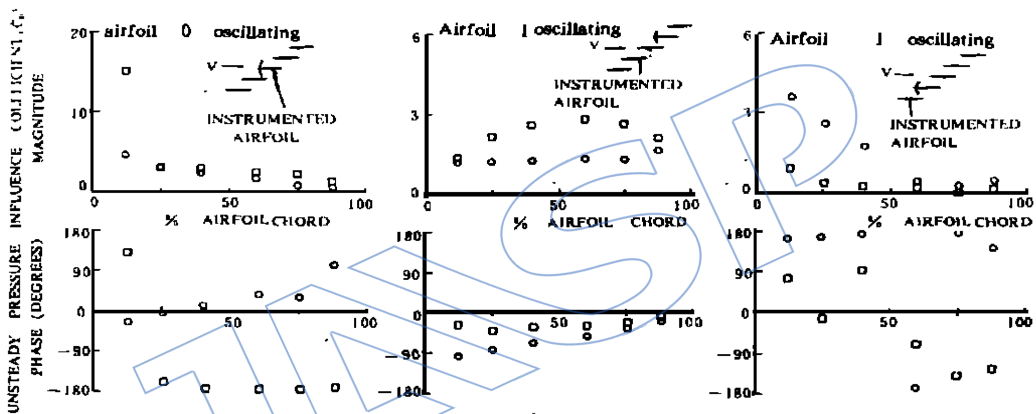

Figure 5. Unsteady pressure influence coefficient $\hat{C}_p^o$ ($Ma = 0.8$, $k = 0.323$, ○—lower □—upper surface)

Fig. 5a and 5b show the unsteady pressure effect on the surfaces of the stationary instrumented reference airfoil due to individually oscillating its nearest neighbors, i.e., individually oscillating the airfoils in Positions + 1 and − 1, respectively. As seen, oscillating the neighboring airfoil has a relatively large effect on the magnitude of the unsteady pressure on the reference airfoil surface nearest to the oscillating airfoil. In particular, Figure 5b shows that oscillating the airfoil located immediately above the reference airfoil results in relatively large unsteady pressure fluctuations over the aft half of the reference airfoil upper surface, with the lower surface pressure coeffcient magnitude nearly constant and a nearly linear variation in the lower surface phase angle. With the oscillating airfoil positioned immediately below the reference airfoil, Fig. 5c shows that there are relatively large pressure fluctuations over the leading quarter of the reference airfoil lower surface, while the upper surface has only a small response in the leading and trailing edge regions, with lower surface oscillations out-of-phase with the motion.

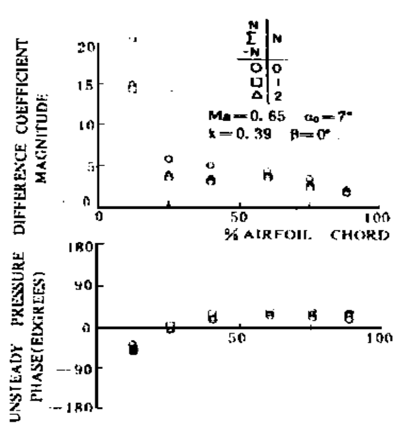

Figure 6. Summation of unsteady pressure influence coefficients

The effect of oscillating the airfoils which are in the + 2 and − 2 positions, i.e., the oscillating airfoils are further distanced from the reference airfoil, is to further reduce the magnitude of the unsteady pressures on the reference airfoil as compared to the previous results where the nearest neighbors were oscillated.

Unsteady Pressure Differences Summation of the unsteady pressure influence coefficients to determine the unsteady pressure difference coefficient is demonstrated in Figure 6. The 0.65 inlet Mach number, 7° incidence, 0.39 reduced frequency data are presented as a dynamic pressure difference coeffcient for $\beta = 0°$ with N specifying the limits of the sum per Equation 1. Thus $N = 0$ corresponds to the self-induced unsteady aerodynamic response. The influence coefficient series is rapidly convergent, with only the reference airfoil and its two immediate neighbors having a singnificant effect on the resulting dynamic pressure differences.

The influence coefficient determined unsteady airfoil surface pressure difference data are correlated with: (1) corresponding data obtained in experiments in which all of the cascaded airfoils are oscillating sumultaneously with $\beta = -90°$, $0°$ and $+90°$, and (2) the classical thin airfoil cascade predictions. The results for an $Ma = 0.65$ and a reduced frequency of 0.39 are presented in Fig. 7 for 0 degrees incidence and in Fig. 8 for 7 degrees of incidence. For $Ma = 0.80$ and a reduced frequency of 0.323, the unsteady pressure difference results are presented in Fig. 9.

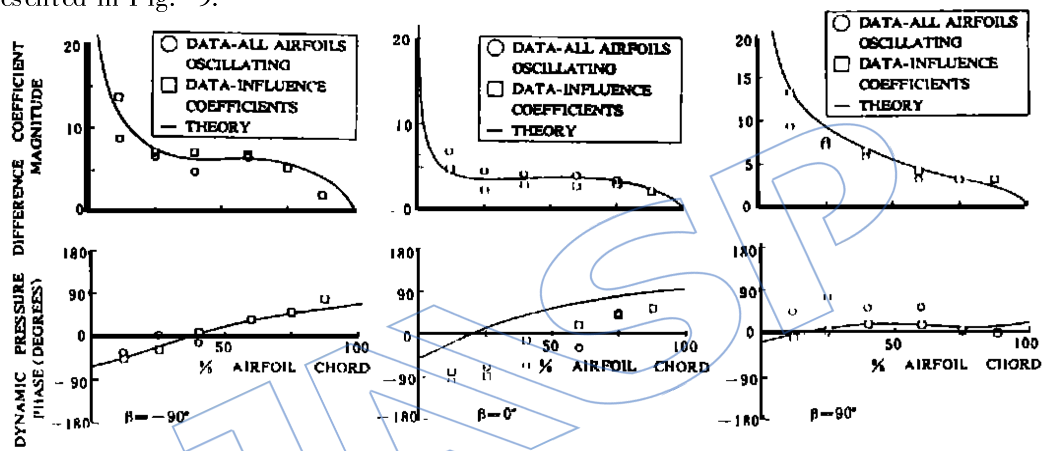

Figure 7. Dynamic pressure difference coefficients ($Ma = 0.65$, $\alpha_0 = 0°$, $k = 0.390$)

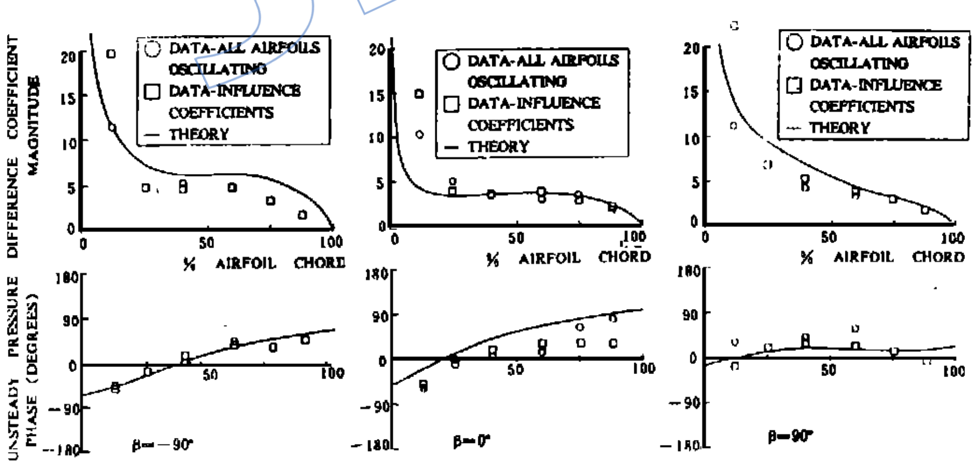

Figure 8. Unsteady pressure difference coefficient distribution ($Ma = 0.65$, $\alpha_0 = 7°$, $k = 0.39$)

With regard to the unsteady difference magnitude data, at $\alpha_0 = 0$, $Ma = 0.65$, the complex unsteady aerodynamic influence coefficient magitude data generally exhibit good correlation with both the oscillating cascade data and the linearized theory. In contrast, at $\alpha_0 = 7°$ with both $Ma = 0.65$ and 0.80, the linearzed theory tends to overpredict the magnitued data. However, for these two cases, there is gnerally very good agreement between the two sets of

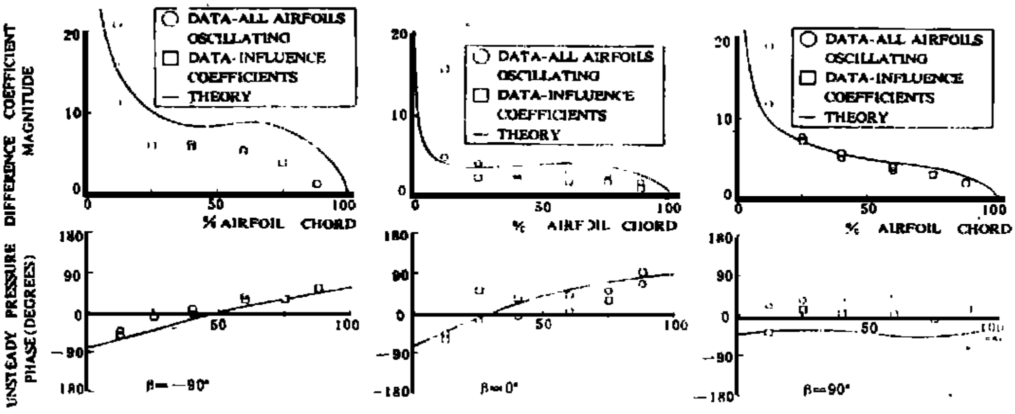

Figure 9. Unsteady pressure difference coefficient distribution ($Ma = 0.80$, $\alpha_0 = 7°$, $k = 0.323$)

experimental magnitude data, with the exception of the leading edge region where the magnitudes of the influence coefficient data are significantly larger than the others. At the lower subsonic Mach number, this is due to a small oscillating separation bubble near the leading edge of the upper surface during the influence coefficient experiments. This separation was first indicated by significant higher harmonic content in the leading upper surface pressure transducer signal, with subsequent steady state flow visualization with Airfoil 0 set at 8.2 degrees of incidence indicating a small separated flow region near the leading edge. At $Ma = 0.80$, the oscillating leading edge shock is the cause of the leading edge data variations.

With regard to the unsteady pressure difference phase data, at $\alpha_0 = 0°$ with $Ma = 0.65$, the phase data are in good agreement with the prediction at $\beta = -90°$. However, for in-phase motions, the phase data are decreased relative to the prediction, with the influence coefficient data centered between the prediction and the oscillating cascade data at 40% and 60% of chord. At $\beta = +90$, the influence coefficient phase data are in good agreement with the prediction, with the oscillating cascade data increased in value.

At $\alpha_0 = 7°$ and $Ma = 0.65$ and 0.80, the −90 degree interblade phase angle influence coefficient data are in good agreement with the all airfoil oscillating data and also the predictions. For in-phase motions, the correlation of these 7 degree incidence phase angle data is good at $Ma = 0.65$, with $Ma = 0.80$ data exhibiting scatter. For $\beta = +90°$ of $Ma = 0.65$, the phase data fall within a fairly narrow band, with the influence coefficient data typically between the prediction and the all airfoil oscillating data. This trend is also evident at $Ma = 0.80$, although there is now more offset among the various results.

SUMMARY AND CONCLUSIONS

Fundamental experiments have been performed in the NASA lewis Transonic Oscillating Cascade Facility to investigate the steady and torsion mode oscillating aerodynamics of a biconvex airfoil cascade. For subsonic and transonic mean flow conditions and realistic high values of reduced frequency, an unsteady aerodynamic influence coefficient technique was developed and utilized in which only one airfoil in the cascade is oscillated at a time and the resulting unsteady pressures measured on the oscillating airfoil and its stationary neighbors. The unsteady aerodynamics of an equivalent cascade with all airfoils oscillating for arbitrary interblade phase angles is then determined by means of a vector summation of these data.

These unsteady aerodynamic influence coeffcient experiments were performed at an inlet Mach number of 0.65 with a reduced frequency of 0.39 at both 0 and 7 degrees of incidence as well as at an inlet Mach number of 0.80 with a reduced frequency of 0.323 at 7 degrees of incidence. The analysis of these unique data and correlation with both the predictions from the unsteady, small perturbation, subsonic flat plate cascade analyses and baseline data obtained in experiments where all of the airfoils are oscillating simultaneously revealed the following:

1. The unsteady aerodynamic influence coefficient series is rapidly convergent. Only the reference airfoil and its two neighbors have a significant effect on the resulting unsteady pressure difference.

2. The unsteady pressure difference magnitude data determined from the influence coefficient experiments generally exhibit good correlation with both the oscillating cascade data and the linearized theory. The primary exception is in the vicinity of the leading edge at $\alpha_0 = 7°$ at both $Ma = 0.65$ " 0.8.

3. The correlation of the unsteady pressure difference phase data determined from the influence coefficient experiments with the oscillating cascade data and the predictions were generally good, but were a function of the interblade phase angle as well as the mean flow conditions.

REFERENCES

[1] Hanamura, Y., Tanaka, H. and Yamaguchi, K., "A Simplified Method to Measure Unsteady Forces Acting on the Vibrating Blades in Cascade", Bulletin of the JSME, Vol. 23, No. 180, June 1980, pp. 880–887.

[2] Davies, M. R. D. and Whitehead, D. C., "Unsteady Aerodynamic Measurements in a Transonic Annular Cascade", Unsteady Aerodynamics of Turbomachines and Propellers, Cambridge University, Cambridge, England, September, 1984, pp. 487–502.

[3] Tanaka, H., Yamamoto, K. and Fujimoto, I., "Unsteady Aerodynamic Response of Cascade Blades in Pitching Oscillation with Flow Separation", Unsteady Aerodynamics of Turbomachines and Propellers, Cambridge University, Cambridge, England, September, 1984, pp. 397–410.

[4] Buffum, D. H., and Fleeter, S., "Investigation of Oscillating Cascade Aerodynamics by an Experimental Influence Coefficient Technique", NASA Technical Memorandum 101313, AIAA Paper 88–2815, July 1988.

[5] Buffum, D. H., and Fleeter, S., "Experimental Investigation of Transonic Oscillating Cascade Aerodynamics", NASA Technical Memorandum 101993, AIAA Paper 89–0321, January 1989.

[6] Szechenyi, E., "Fan Blade Flutter-Single Blade Instability or Blade to Blade Coupling?", ASME Paper 85-GT-216, March 1985.

[7] Burgess, J. C., "On Digital Spectrum Analysis of Periodic Signals", Journal of the Acoustical Society of America, Vol. 58, No. 3, September 1975, pp. 556–567.

[8] Smith, S. N., "Discrete Frequency Sound Generation in Axial Flow Turbomachines", Cambridge University Report CUED/A-Turbo/TR29, 1971.

[9] Fleeter, S., "Fluctuating Lift and Moment Coefficients for Cascaded Airfoils in a Nonuniform Compressible Flow", AIAA Journal of Aircraft, Vol. 10, No. 2, February 1973, pp. 93–98.